Biomass Conversion and Biorefinery
https://doi.org/10.1007/s13399-024-05314-w

ORIGINAL ARTICLE

Synthesis of silver nanoparticles using *Alchemilla vulgaris* and *Helichrysum arenarium* for methylene blue and 4-nitrophenol degradation and antibacterial applications

Havva Tutar Kahraman[1]

Received: 20 October 2023 / Revised: 2 January 2024 / Accepted: 12 January 2024

Abstract
This study aimed to evaluate the concept of green synthesis of metallic nanoparticles (silver nanoparticles, AgNPs) by plant extracts without using any toxic or hazardous materials. *Alchemilla vulgaris* (AV) and *Helichrysum arenarium* (HA) are used as capping and reducing agents to synthesize AgNPs (as coded AV-AgNPs and HA-AgNPs). Both synthesized AgNPs were characterized by UV–visible spectrophotometry, Fourier transform infrared spectroscopy (FT-IR), X-ray diffraction (XRD), and transmission electron microscope (TEM). The results of characterization exhibited that AgNPs were successfully synthesized. They are highly well-dispersed, mostly spherical shape with an average size 15–20 nm. Catalytic reduction of methylene blue (MB) and 4-nitrophenol (4-NP) was assessed using synthesized AgNPs as nano-catalysts in the presence of $NaBH_4$. The catalytic activity of the synthesized AgNPs revealed significant results in terms of degradation of MB and 4-NP to 4-AP (4-aminophenol). The reduction reactions of MB and 4-NP happen within 6–7 min using synthesized AV-AgNPs and HA-AgNPs in the presence of $NaBH_4$. According to the reusability analysis, synthesized AgNPs demonstrated excellent degradation performances by the more than 94% removal efficiency maintained after five reuse cycles. In addition, antibacterial activities of AgNPs were investigated against *Escherichia coli* (*E. coli*; Gram-negative bacteria) and *Staphylococcus aureus* (*S. aureus*; Gram-positive bacteria) by using quantitative well-diffusion method and the inhibition zones were determined using Mueller–Hinton agar (MHA) media. AV-AgNPs and HA-AgNPs showed strong antibacterial activities against *E. coli* with in inhibition zone diameters 25.5 and 25 mm, respectively. AV-AgNPs and HA-AgNPs were also extremely effective on *S. aureus* with high inhibition zone values of 22 and 24 mm, respectively. Finally, the fabricated silver nanoparticles could be excellent candidates for the separation of hazardous materials.

Keywords Green synthesis · Antibacterial · Silver nanoparticles · Methylene blue · Nitrophenol · Catalytic degradation

1 Introduction

Metal nanoparticles (mNPs) of varying sizes demonstrate unique electronic, magnetic, catalytic, and optical properties that are different from those of bulk metals. They have many fascinating properties, the size-dependent metal to nonmetal transition being an important one [1–5]. Thus, they have been used in many interesting different applications like optoelectronics, chemical and biochemical sensors, catalysis, and biomedical sciences [6, 7]. Bare metal nanoparticles can be prepared by employing physical and chemical methods for a long time [8]. However, the development of efficient methods has been investigated in order to find an eco-friendly technique for the fabrication of well-characterized mNPs. Biosynthesis of mNPs is an environmentally friendly method without the need for any toxic chemicals. In this context, bacteria, yeast, fungi, algae, actinomycetes, and plants are used for bioreduction of metals [9]. Among these organisms, plant extract has received more attention as a best candidate to other bioreduction agents [10, 11]. Because, using plant extracts is a very cost-effective method and valuable alternative for the production of mNPs in the absence of chemicals [12]. Combination of biomolecules (e.g., amino acids, polysaccharides, proteins, enzymes, vitamins, and organic acids) found in plant extracts plays important roles in both stabilization and reduction of metals. This procedure,

✉ Havva Tutar Kahraman
hkahraman@ktun.edu.tr

[1] Present Address: Department of Chemical Engineering, Konya Technical University, 42250 Konya, Turkey

Published online: 20 January 2024

called green synthesis, has shown great potential in generation of mNPs [13]. This technique mainly fabricates nanoparticles using reducing and capping agents present in plant extracts [14, 15].

Silver nanoparticles (AgNPs) are well-known in nanotechonology due to their remarkable optical, electrical, and antimicrobial properties [16, 17]. Silver compounds have been applied as antimicrobial agents since ancient times. They are preferable for their broad-spectrum antibacterial activity against Gram-positive and Gram-negative bacteria, fungi, protozoa, and certain viruses [18]. Moreover, AgNPs are widely used for photodegradation process as catalysts with high large surface area to volume ratio [19].

Mass release of hazardous substances into the environment is a rising problem with the development of industrialization. It has resulted in a significant rise in dyes, insecticides, phenols, and other organic contaminants with potentially toxic by-products. Nitrophenols are considered one of the most ubiquitous pollutants in wastewaters [20, 21]. Similarly, a cationic diazine dye such as methylene blue (MB) is widely used in various industrial applications [22]. Therefore, efficient strategies are the current international need for extracting these toxins from industrial wastewater [23]. Chemical techniques such as oxidation and reduction; physical methodologies such as precipitation, adsorption, and reverse osmosis; and biological methods such as aerobic and anaerobic intervention have all been often applied to clean organic pollutant containing wastewaters. Photocatalytic degradation is one of the methods for water purification. Nowadays, biosynthesized nano-catalysts are widely used for the effective removal of contaminants [24, 25].

In this perspective, the novelty of this work appeared on present fabrication AgNPs using plant extracts via green synthesis process, as an eco-friendly nano-catalyst for 4-NP and MB degradation. For this purpose, we used the extracts from *Alchemilla vulgaris* and *Helichrysum arenarium to* synthesize AgNPs (namely coded as AV-AgNPs and HA-AgNPs). The reaction conditions such as temperature, pH, and time on the synthesis of AgNPs were investigated by using a UV–Vis spectrophotometer. The synthesized nanoparticles were analyzed using transmission electron microscopy (TEM), X-ray diffraction (XRD), and Fourier transform infrared (FT-IR) spectroscopy. AgNPs fabricated in this work were used as such to investigate the catalytic potential in the reduction of methylene blue (MB) and 4-nitrophenol by $NaBH_4$. Moreover, the antibacterial activities of synthesized AgNPs were also investigated. Thus, the newly synthesized nanoparticles not only remove organic pollutants from waste water but also hinder the growth of bacteria in water.

2 Experimental

2.1 Materials

All chemicals in this work were used as received and without further purification. Water used for all experimental preparations was Milli-Q grade (18.2 MΩ at 25 °C). Silver nitrate was purchased from Sigma-Aldrich, 4-nitrophenol from Fluka, and sodium borohydride from Sigma-Aldrich. NaOH (analytical reagent grade) was purchased from Sigma-Aldrich used to prepare 4-NP solution. *Alchemilla vulgaris* (AV) and *Helichrysum arenarium* (HA) were purchased from herbal market in Konya, Turkey.

2.2 Synthesis of AgNPs

In the first stage, plant extracts were obtained to synthesize silver nanoparticles by green synthesis method. *Alchemilla vulgaris* (AV) and *Helichrysum arenarium* (HA) were washed with distilled water until impurities were removed. Ten grams of plants were weighed and immersed in 100 mL of distilled water in Erlen-Mayer, were heated to 60 °C during 20 min. After this step, the plant extract solutions were mixed using magnetic stirrer at room temperature for 24 h. Then, plant extracts were filtered by using filter paper and supernatants were collected and kept at 4 °C for the synthesis of nanoparticles.

In the second step of the synthesis process, certain plant extracts were added to 0.01 M $AgNO_3$ solution under continuous stirring at room temperature to obtain HA-AgNPs and AV-AgNPs. Stirring was performed until the visible color changing was occurred. Then, the precipitated AgNPs were separated by centrifugation method from aqueous medium. Synthesis of AgNPs was determined by using UV–visible spectrophotometer. This experimental section gives a confirmation data about the characteristic absorbance of AgNPs around 400–450 nm.

2.3 Characterization of AgNPs

TEM analysis was carried out for the confirmation of AgNPs size and shapes, and elemental mapping and compositional analysis were done by EDX. TEM images were used to generate size distribution histograms of AgNPs using ImageJ software, and the resulting histograms were created in OriginPro 2018. Fourier transformed infrared (FT-IR) spectra of active functional groups were detected with Bruker Vertex-70 Fourier transform infrared spectrophotometer. The data were recorded in the range of 4000–400 cm^{-1}. Effects of the parameters on the formation of AgNPs were interpreted by using UV–visible spectrophotometer. UV–visible

analysis was performed between 200 and 800 nm. Additionally, both HA-AgNPs and AV-AgNPS were examined by X-ray diffractometer (Bruker D8 Advance) operated at 40 kV and 35 mA by means of Cu Kα radiation.

2.4 Optimization of AgNPs synthesis parameters

The synthesis of nanoparticles is very sensitive and depends on important parameters. These parameters can be mentioned as follows; reaction time, pH, and temperature of the reaction medium. Since these parameters affect the nanoparticle size, shape, and agglomeration of the particles, we have tried to optimize the parameters for efficient synthesis of AgNPs. For the optimization of pH, pH of the solutions was adjusted to 5, 7, and 9 by keeping $AgNO_3$ and plant extract volume in the ratio of 1:1. Different time durations, i.e., 1 min, 10 min, 30 min, 1 h, 2 h, 3 h, 5 h, 6 h, 24 h, were applied to optimize the reaction time (keeping the parameters as follows: $AgNO_3$ and plant extract volume in the ratio of 1:1, room temperature, pH: 5). Besides this, various temperature conditions (25℃, 40℃, and 60℃) were performed by keeping other parameters fixed for synthesis reaction.

2.5 Catalytic reaction

The UV–visible spectrophotometer was used to monitor the progress of catalytic degradation of MB and 4-NP. The degradation of MB and 4-NP was observed via the absorption spectra obtained using spectrophotometer. The catalytic behavior of synthesized AgNPs (HA-AgNPs and AV-AgNPs) was investigated for MB and 4-NP, separately. This analysis was performed using the reduction of 4-NP to 4-AP (4-aminophenol) as a model reaction in the presence of $NaBH_4$ as a reducing agent.

Catalytic reducing reaction was carried out under specific circumstances in two sets. In the first set, 1 mL of 0.01 M $NaBH_4$ was mixed with 1 mL of 0.002 M MB solution in the absence of AgNPs and UV–vis spectra have been used at orderly interval of time. For the second set, 5 mg of HA-AgNPs and AV-AgNPs were added to the solutions mentioned as before. Similar procedure was employed to monitor the degradation of 4-NP. Methylene blue has an absorption peak at 665 nm with a shoulder at 610 nm. 4-NP solution mixed with $NaBH_4$ presents an absorption peak at around 400 nm.

Reusability of synthesized AgNPs was evaluated by performing a recycling experiment. AgNPs were centrifuged and separated after degradation processes and washed with DI water thoroughly. These cleaned and dried AgNPs were reused in degradation processes and degradation performances were calculated after each cycle.

2.6 Antibacterial activities of AgNPs

Antibacterial activities of AgNPs were investigated against *Escherichia coli* ATCC 25922 (Gram-negative bacteria) and *Staphylococcus aureus* ATCC 25923 (Gram-positive bacteria) by using quantitative well-diffusion method. The inhibition zones were determined using Mueller–Hinton agar (MHA) media. In particular, fresh bacterial cultures (10^8 CFU/mL) were applied on the surface of media. Then, HA-AgNPs and AV-AgNPs (0.10 mg/mL) were added and allowed to diffuse for 1 h and incubated at 37 °C for 24 h. Finally, diameters of inhibition zones for each AgNPs were determined in three replicates [26].

3 Results and discussions

3.1 TEM analysis

The dimensions and physical appearances of synthesized AgNPs were confirmed by TEM analysis. The particle size of generated HA-AgNPs was found in the range of 5–40 nm. As seen in Fig. 1, the average particle size is around 20 nm for HA-AgNPs. Similarly, the particle size of fabricated AV-AgNPs was measured in the range of 1–40 nm and can be reported that average size is around 15 nm. Figure 2 shows the detailed images of synthesized AV-AgNPs.

The representative images of HA-AgNPs and AV-AgNPs showed the morphology of the nanoparticles were found to be roughly spherical in shape. Huang et al. has reported that the mNPs with spherical shape show well thermodynamic stability due to the protection by a sufficient amount of biomolecules [27, 28]. Additionally, it can be suggested that these fabricated AgNPs, having small sizes and monodispersed structures, can be used in waste water treatment.

The size distribution was analyzed using ImageJ software package. For this purpose, first images of Fig. 1 and Fig. 2 obtained from TEM analysis (inset images in Fig. 3) were chosen to create size distribution histograms of HA-AgNPs and AV-AgNPs, respectively. It is observed that HA-AgNPs have a good dispersion with calculated average particle size diameter of 18.79 nm. It is noticeable that the size and distribution of the AV-AgNPs are not uniform as HA-AgNPs. According to this result, stirring step of AV-AgNPs synthesis process can be prolonged to obtain more homogenous structure for further studies.

3.2 FT-IR analysis

The FT-IR spectra of HA-AgNPs and AV-AgNPs were depicted in Fig. 4 a and b respectively. This analysis was carried out to procure the chemical composition of the surface of the AgNPs and the molecular composition of

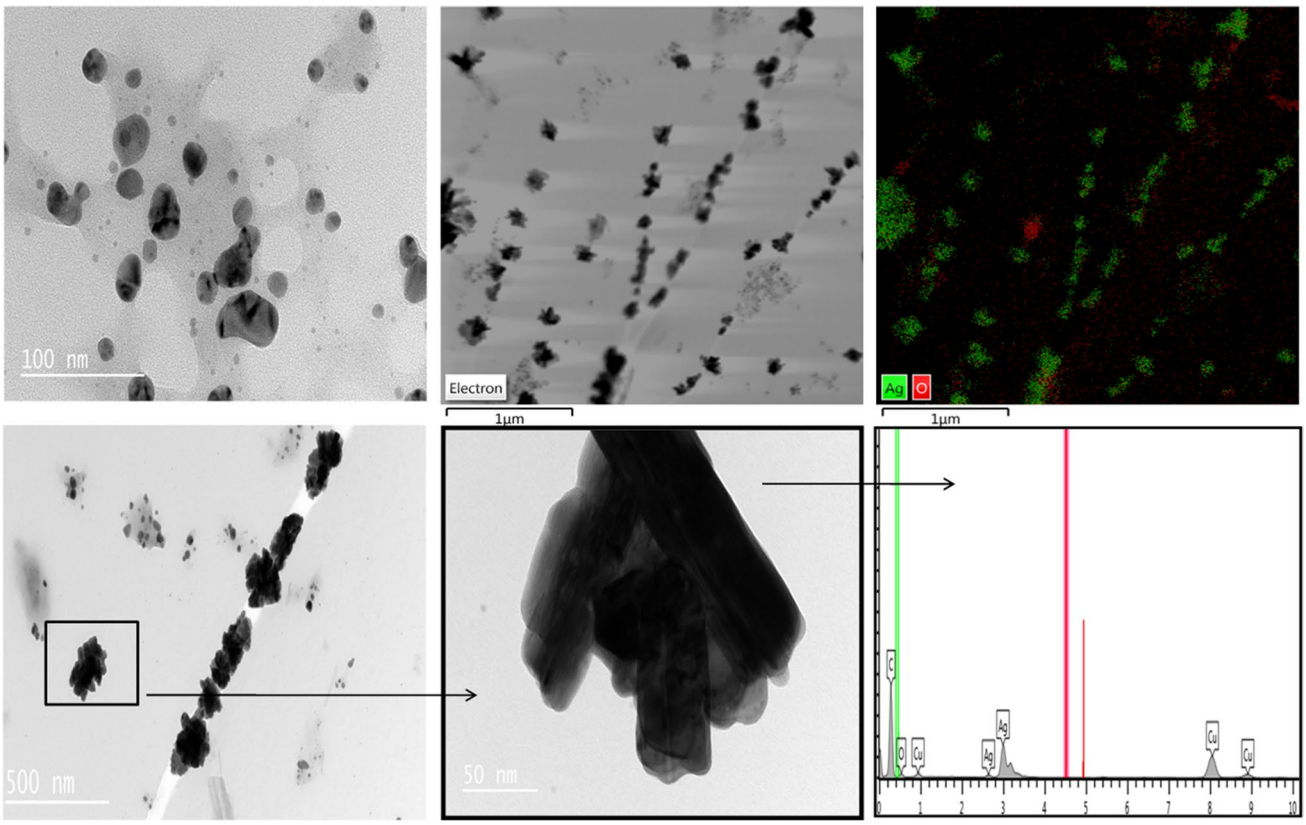

Fig. 1 TEM images of HA-AgNPs

the capping agents on the nanoparticles [29]. FT-IR results of AgNPs showed that the band at around 3350 cm^{-1} corresponds to –OH stretching vibration caused by phenol compounds. The band at 2958 cm^{-1} corresponds to the C-H stretching vibration. The carbonyl group was detected at 1715 cm^{-1}. The carbonyl groups showed the presence of flavanones or terpenoids that are adsorbed on the surface of metal nanosized particles [30]. Carboxyl groups attached to the amide band can be explained with the band at 1645 cm^{-1} [31]. The band at 1363 cm^{-1} showed the vibrations of aromatic amines.

The band at 1072 cm^{-1} shows C–N stretching vibrations of aliphatic amines [32]. Investigation of the chemical components of the surface of the synthesized AgNPs specified the existence of amides, carboxyl, amino groups, and poly phenols in HA-AgNPs and AV-AgNPs. These mentioned organic components in plant extracts can attribute to the reduction of $AgNO_3$ and the stabilization of AgNPs by the surface bound by the organic molecules. Consequently, FT-IR analysis confirmed that plant extracts have a capability for the reduction of $AgNO_3$ and the stabilization of AgNPs [30].

3.3 X-ray diffraction

This analysis was performed to evaluate the crystal structures of synthesized AgNPs. Figure 5 shows the XRD pattern of HA-AgNPs and AV-AgNPs. A number of Bragg reflections with 2θ values of 39.40, 44.51, 62.22, and 76.10 matching to the (111), (200), (220), and (311) set of lattice planes, respectively, in Miller indices. The resulting structures are compared with the standard silver XRD pattern reported by joint committee for powder diffraction set (JCPDS Card No: 04–0783), confirming a face centered cubic geometry of silver. The presence of sharp structural peaks in pattern demonstrates that generated AgNPs were nanocrystalline structure. These XRD results are in agreement with previous reports of synthesized AgNPs using green methods [33–37]. Then, the Debye–Scherrer equation was applied to probe the crystalline structure of AgNPs. The calculated average particle size is 15–30 nm for synthesized AgNPs.

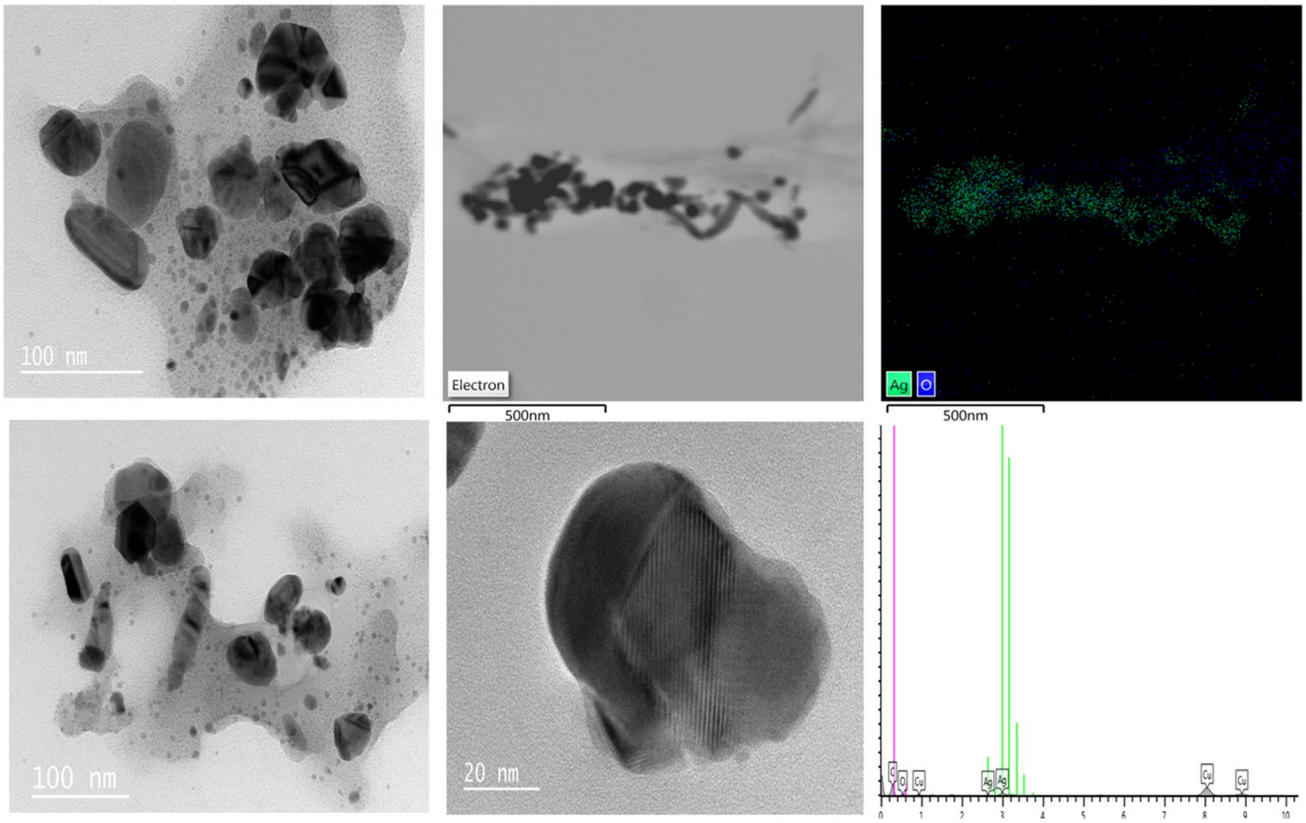

Fig. 2 TEM images of AV-AgNPs

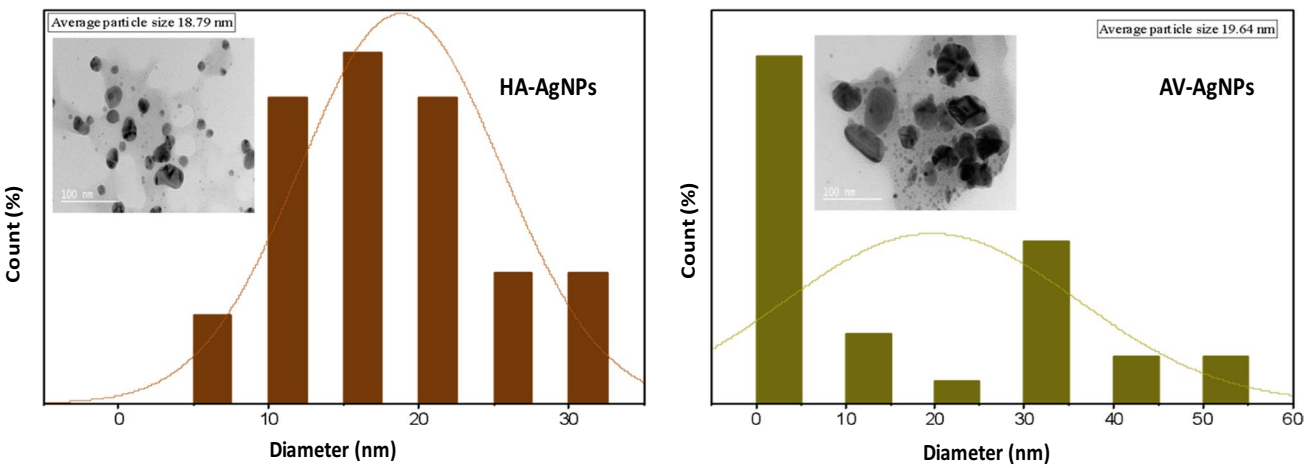

Fig. 3 Size distribution histograms of AgNPs

3.4 Optimization of reaction parameters

As shown in Fig. 6, effects of the different pH values, variable time, and temperature intervals were examined in this part of the study. In the optimization of the synthesis reaction of AgNPs using plant extracts, it was demonstrated that the pH of solutions, reaction time, and temperature have a remarkable effect on the characteristic absorbance indicating the formation of silver AgNPs, which agrees with other previously reported studies [38–40].

The effect of pH on the absorbance profile of $AgNO_3$-plant extract solution is shown in Fig. 6 a and b. The pH adjustment

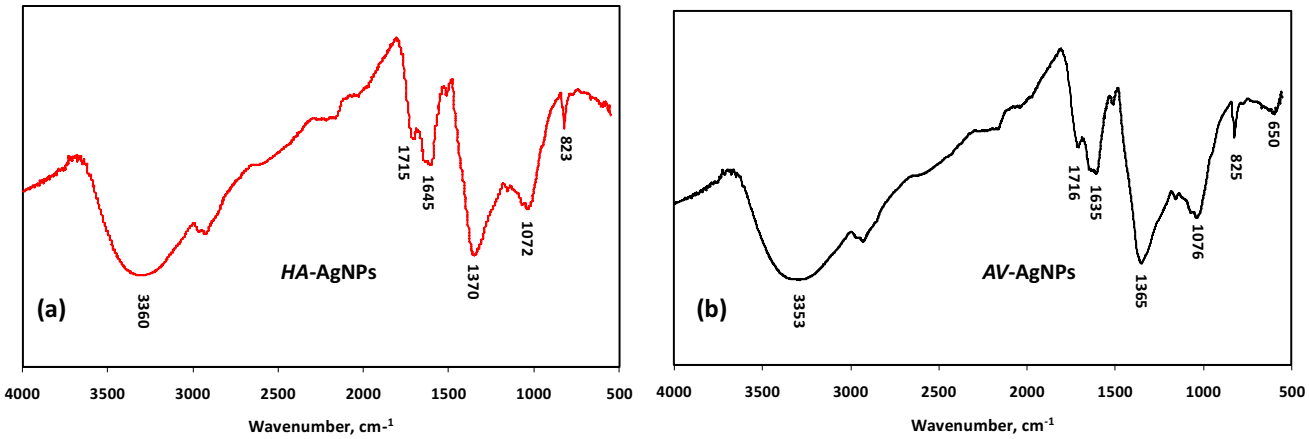

Fig. 4 FT-IR spectra of HA-AgNPs and AV-AgNPs

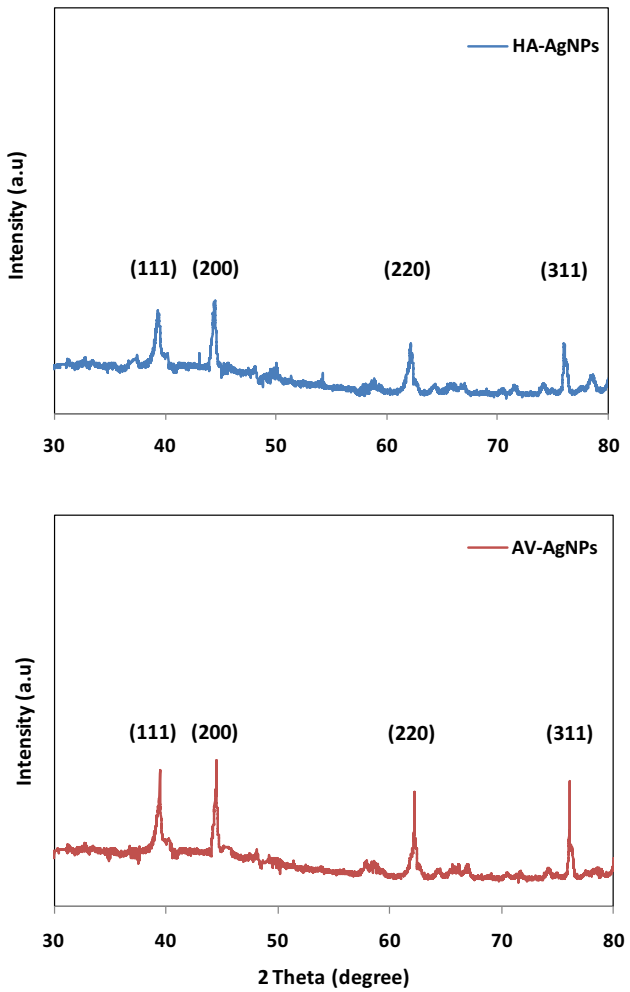

Fig. 5 XRD patterns of HA-AgNPs and AV-AgNPs

significantly influenced the reduction of Ag^+ ion to Ag indicating the color change to dark brown. The progress of synthesis process depends on the role of phyto chemicals in reaction medium that affected by the pH. Moreover, pH of medium affects the AgNPs synthesis by changing the charges of biomolecules [41]. The absorbance peak at 412 nm increased with the decrease of pH for both AgNPs formation. pH:5 was suitable value for the efficient synthesis of AgNPs.

Figure 6 c and d shows the results of effect of the reaction time on absorbance profiles of reduction process to Ag. As seen from the figure, the resonance plasmon occurred at approximately 400–420 nm with increasing reaction time for both reactions. As a result of the applied time interval, 24 h and 6 h were suitable for HA-AgNPs and AV-AgNPs, respectively. The increase of intensity of the peak was observed without a change in position, which shows that the nucleation process was still going until 24 and 6 h for HA-AgNPs and AV-AgNPs. Due to the slightly shift of the absorbance band of AV-AgNPs, 6 h was adequate for synthesis. Because, the observation of widening or shift of the plasmon band explains that there may be an agglomeration or increase in nanoparticle size [15, 38]. Furthermore, temperature plays an important role in the production of AgNPs. As seen from the Fig. 6 e and f, 25℃, 40℃, and 60℃ were applied during the synthesis reaction. The highest intensity peak was observed at 60℃ for HA-AgNPs and AV-AgNPs. This absorbance pattern is in good agreement with the reported profiles in the literature for the AgNPs synthesized by green methods [42, 43].

3.5 Catalytic applications

3.5.1 Catalytic degradation of MB

Catalytic activities of HA-AgNPs and AV-AgNPs for the degradation of MB were monitored using UV–visible

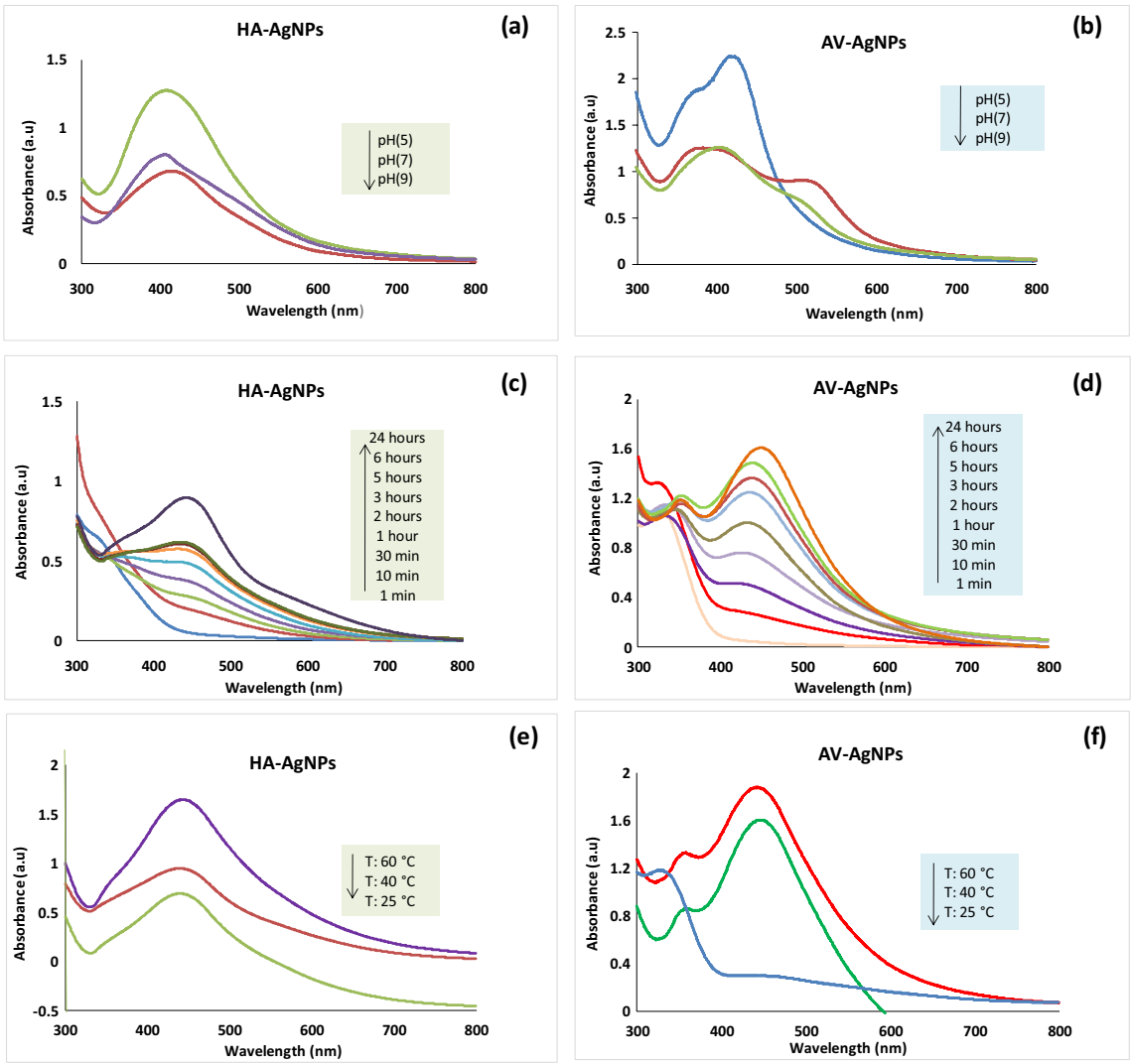

Fig. 6 Optimization of the HA-AgNPs and AV-AgNPs synthesis reaction parameters

spectrophotometer. The results for MB degradation were presented in Fig. 7. MB has an absorption peak at 665 nm with a shoulder at 610 nm. MB degradation was also observed by color change and recorded as picture inset Fig. 7 b. In first step, the degradation of MB was experienced using $NaBH_4$ in the absence of AgNPs. As seen from the Fig. 7 a, the degradation process is almost not observed without using AgNPs. The absorption peaks were slightly decreased after 60 min. However, the absorption spectrums showed the decreased peaks upon different time intervals for AV-AgNPS and HA-AgNPs as seen in Fig. 7 b and c. Degradation of MB is known from the gradual decrease of absorbance curve approaching the base line [44]. The characteristic peak of MB was completely disappeared after 6–7 min in the presence of AgNPs. AgNPs were catalyzed the degradation process successfully as reported in previous studies [41, 45]. Furthermore, peaks at around 400 nm can be concerned with absorbance bands of AgNPs for both absorbance profiles. Additionally, catalytic reduction leads to convert MB into Leuco-methylene blue which is colorless and less toxic product. The production of Leuco-MB, was occurred via the transformation of C = N bonds of the MB molecule into the NH bonds by the electrons on the AgNPs [46, 47].

Moreover, reusability is a very important criterion for determining the practical application of nanoparticles. The degradation percentage of each cycle was calculated based on Eq. (1).

$$\propto = \frac{Co - Ct}{Co}.\%100 \tag{1}$$

where C_o is the initial concentration and C_t is the concentration at the termination stage [48]. The efficiency of each cycle was determined at termination time of 10 min. Figure 7d shows the reusability performances of AgNPs for

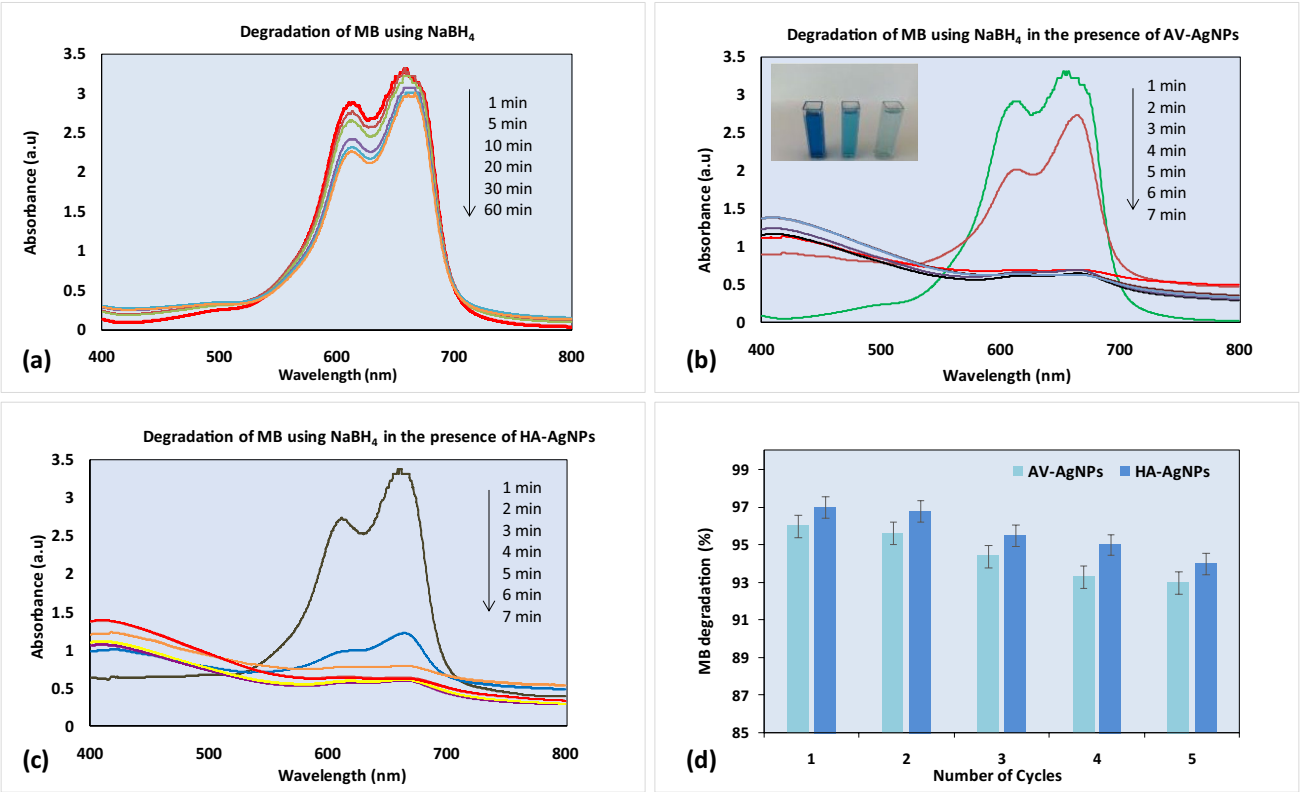

Fig. 7 MB degradation using $NaBH_4$ in the absence of any AgNPs (**a**), degradation of MB using $NaBH_4$ in the presence of AV-AgNPs and HA-AgNPs (**b**, **c**), number of cycles for AV-AgNPs and HA-AgNPs (**d**)

consecutive cycles. The recycled nanoparticles showed satisfying photocatalytic activities up to five cycles with high efficiencies under the same reaction conditions. The percentages for both AgNPs remain above 96% up to cycle three, and it has been concluded that the efficiencies were still high for the 5 cycles with 94% degradation percentage. These results demonstrate that synthesized AgNPs protect their catalytic activities up to five cycles without losing their performances.

3.5.2 Catalytic degradation of 4-NP

In recent years, the catalytic degradation of 4-NP to 4-AP by $NaBH_4$ in the presence of mNPs has turn out to be of great concern [49]. Here, synthesized AV-AgNPs and HA-AgNPs were utilized as catalysts for 4-NP degradation reaction. Figure 8a shows the degradation of 4-NP using $NaBH_4$ in the absence of any AgNPs. As seen from the figure, there is a negligible shift in absorbance after 60 min. The spectrum demonstrates that the original absorption spectrum did not alter significantly after one hour. Though the reduction of 4-NP by $NaBH_4$ is a thermodynamically possible reaction, without a catalyst, it is kinetically limited [50]. In Fig. 8 b and c, decreased absorbance peaks were recorded in the presence of AV-AgNPs and HA-AgNPs prominently. With the introduction of small amount of AgNPs, the absorption intensities of 4-NP at around 400 nm diminished rapidly with increasing time. This catalytic phenomenon was also observed through the naked eye as the yellow color of the solution turned colorless after 6 min (Fig. 8 c). As we mentioned in previous section, the absorption peaks tend to approach to the base line as seen in the absorbance graph, when the reduction proceed to the end. As shown in figure, the characteristic peaks were completely disappeared after 6 min for AV-AgNPs and HA-AgNPs. Absorption peaks around 300 nm indicate the formation of 4-AP for both degradation profiles [51–53].

Furthermore, Fig. 8 d shows the reusability performances of AgNPs for consecutive cycles. The percentages for both AgNPs remain above 96% up to cycle three, and it has been concluded that the efficiencies were still high for the 5 cycles with 93% degradation percentage. AgNPs showed effective photocatalytic activities up to five cycles with high efficiencies under the same reaction conditions. The reusability profiles of AV-AgNPs and HA-AgNPs were recorded similarly to the reusability results of MB degradation.

Consequently, the reaction times found for the degradation of MB and 4-NP were very similar and significantly

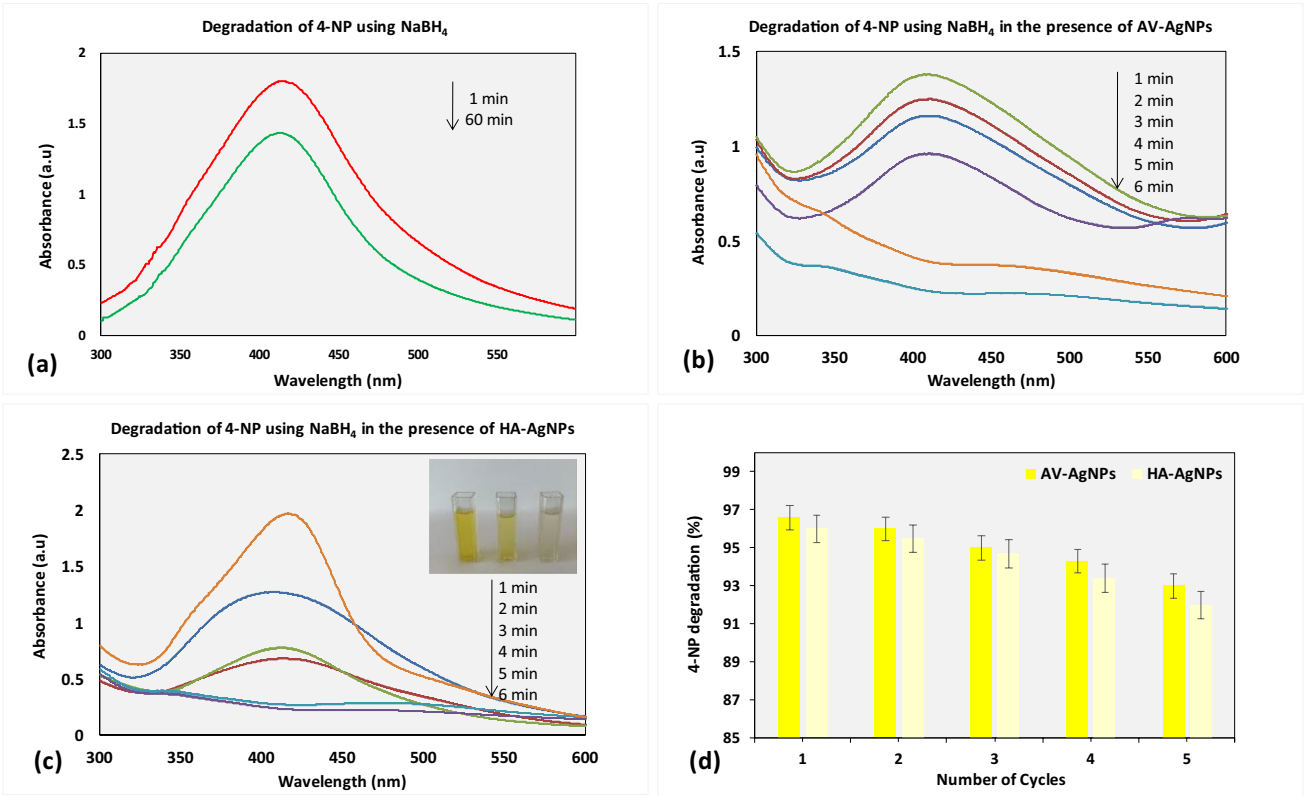

Fig. 8 4-NP degradation using $NaBH_4$ in the absence of any AgNPs (**a**), degradation of 4-NP using $NaBH_4$ in the presence of AV-AgNPs and HA-AgNPs (**b**, **c**), number of cycles for AV-AgNPs and HA-AgNPs (**d**)

lower than in earlier reports [41, 52, 54–57]. AV-AgNPs and HA-AgNPs have high rate of catalytic reduction capabilities, with a reaction time less than 5 min. It can be reported that almost complete degradation of MB and 4-NP happened at the time of 7 min with both AgNPs. In terms of reusability, the performance of HA-AgNPs was measured to be slightly higher in MB degradation, while the performance of AV-AgNPs was observed to be higher in 4-NP degradation. Based on these results, it can be concluded that synthesized AgNPs in present study can take a role as efficient photocatalysts in dye degradation processes.

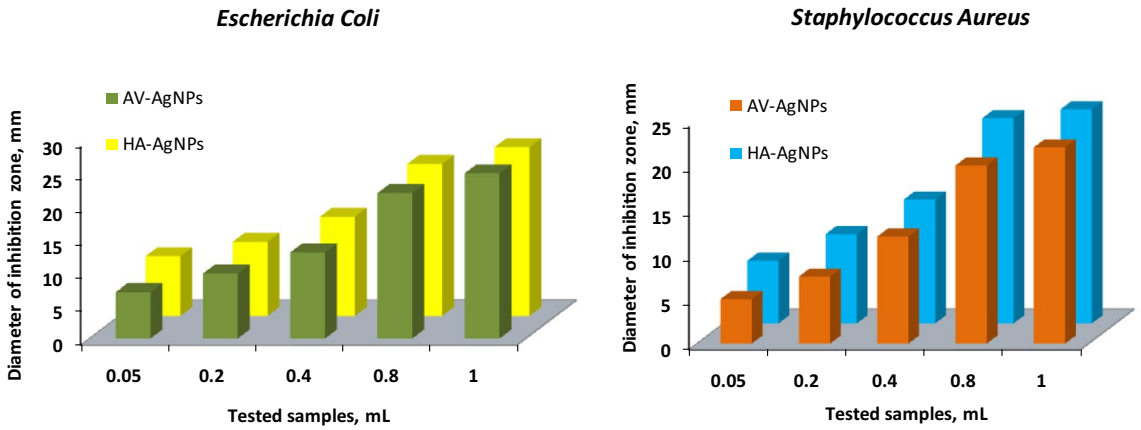

Fig. 9 Antibacterial activities of AgNPs against *E. coli* and *S. aureus* bacteria

3.6 Antibacterial activities of AgNPs

The antibacterial activities of newly synthesized silver nanoparticles (HA-AgNPs and AV-AgNPs) were assessed against both *S. aureus* and *E. coli* bacteria by an agar well-diffusion method. The experiments were carried out in triplicate and the average values were evaluated and illustrated in Fig. 9.

The synthesized AgNPs had impressive antibacterial activities against the two bacteria under study. Zone diameters of inhibition were measured versus different concentrations of AgNPs. The zones of inhibition against *E. coli* bacteria were found to be 9, 11.2, 15, 23, and 25.5 mm for HA-AgNPs; 7, 9.8, 13, 22, and 25 mm for AV-AgNPs with 0.05, 0.2, 0.4, 0.8, and 1 mL AgNPs concentrations. The diameter of inhibition zones of *S. aureus* bacteria were determined to be 7, 10, 13.9, 23, and 24 mm for HA-AgNPs; 5, 7.5, 12, 20, and 22 mm for AV-AgNPs in the same nanoparticles concentration range. As seen from the results, antibacterial activities of AgNPs increased with an increase in AgNPs concentration, which could be attributed to a more significant quantum of nanoparticles available to kill the microorganisms [15]. Similarly, antibacterial inhibition zone diameter for plant-based AgNPs was reported as 17–18 mm in literature [58].

According to our best knowledge, increased surface area of smaller AgNPs are successful in attaching to the surface of bacteria cell wall [59]. Besides, smaller AgNPs with large surface area give more bacterial effect than the larger AgNPs. Several studies propose that it is also possible that AgNPs not only interact with the surface of membrane, but can also penetrate inside the bacteria [60, 61]. This phenomenon is compatible with the results obtained from our experiments. It can be claimed that HA-AgNPs show a more homogenous structure consisting smaller particles than AV-AgNPs. Similar results are reported in literature [26, 59]. Based on these results, AgNPs fabricated in this work, can be used in antibacterial applications without losing high efficiency.

4 Conclusions

In this study, we have demonstrated that a concept to fabricate AgNPs via green synthesis method. Two different AgNPs were successfully synthesized using *Alchemilla vulgaris* and *Helichrysum arenarium* extracts. This green synthesis method is considered a simple, cost-effective, fast, and eco-friendly method to generate metallic nanoparticles. Synthesized AgNPs were characterized by using UV–Vis spectroscopy, X-ray diffraction, FT-IR, and TEM. The obtained results showed the presence of chemical groups that could take a role as either reducing agents or capping agents for enhancing the properties of AgNPs. Regarding to TEM and XRD results, it can be concluded that both HA-AgNPs and AV-AgNPs are highly well-dispersed, mostly spherical with an average size 15–20 nm. After that, catalytic reduction of MB and 4-NP was assessed using synthesized AgNPs as nano-catalysts in the presence of $NaBH_4$. The catalytic activity of the synthesized AgNPs revealed significant results in terms of degradation of MB and 4-NP to 4-AP. The reduction reactions of MB and 4-NP happen within 6–7 min using synthesized AV-AgNPs and HA-AgNPs in the presence of $NaBH_4$. According to the reusability analysis, synthesized AgNPs demonstrated excellent degradation performances by the more than 94% removal efficiency maintained after five reuse cycles. In addition, in terms of antibacterial activity behavior, both HA-AgNPs and AV-AgNPs were tested against Gram (+) and Gram (−) bacteria. The outcomes of this analysis confirm a more significant antibacterial effect of the synthesized AgNPs. When the inhibition zone diameters are examined, HA-AgNPs displayed much better antibacterial acitivity than AV-AgNPs with a small difference. Ultimately, both HA-AgNPs and AV-AgNPs are promising candidates for the application in catalytic degradation of organic pollutants from wastewater.

Funding Open access funding provided by the Scientific and Technological Research Council of Türkiye (TÜBİTAK).

Data availability All data and materials used for the reported work are all reported in the manuscript.

Declarations

Ethics approval and consent to participate Not applicable.

Conflict of interest The author declares no competing interests.

References

1. Aravind M, Ahmad A, Ahmad I, Amalanathan M, Naseem K, Mary SMM, Zuber M (2021) Critical green routing synthesis of silver NPs using jasmine flower extract for biological activities and photocatalytical degradation of methylene blue. J Environ Chem Eng 9(1):104877
2. Anis M, Hashemi SH, Nasri A, Sajjadi M, Eslamipanah M, Jaleh B (2022) Decorated ZrO2 by Au nanoparticles as a potential

nanocatalyst for the reduction of organic dyes in water. Inorg Chem Commun 141:109489
3. Nasri A, Jaleh B, Nezafat Z, Nasrollahzadeh M, Azizian S, Jang HW, Shokouhimehr M (2021) Fabrication of g-C3N4/Au nanocomposite using laser ablation and its application as an effective catalyst in the reduction of organic pollutants in water. Ceram Int 47(3):3565–3572
4. Ahmad PT, Jaleh B, Nasrollahzadeh M, Issaabadi Z (2019) Efficient reduction of waste water pollution using GO/γMnO2/Pd nanocomposite as a highly stable and recoverable catalyst. Sep Purif Technol 225:33–40
5. Nezafat Z, Mohazzab BF, Jaleh B, Nasrollahzadeh M, Baran T, Shokouhimehr M (2021) A promising nanocatalyst: upgraded Kraft lignin by titania and palladium nanoparticles for organic dyes reduction. Inorg Chem Commun 130:108746
6. Mody VV, Siwale R, Singh A, Mody HR (2010) Introduction to metallic nanoparticles. J Pharm Bioallied Sci 2(4):282
7. Rudge S, Peterson C, Vessely C, Koda J, Stevens S, Catterall L (2001) Adsorption and desorption of chemotherapeutic drugs from a magnetically targeted carrier (MTC). J Control Release 74(1–3):335–340
8. Thacharon A, Jang WS, Kim J, Kang J, Kim YM, Kim SW (2022) Non-oxidized bare metal nanoparticles in air: a rational approach for large-scale synthesis via wet chemical process. Adv Sci 9(26):2201756
9. Saravanan A, Kumar PS, Karishma S, Vo DVN, Jeevanantham S, Yaashikaa PR, George CS (2021) A review on biosynthesis of metal nanoparticles and its environmental applications. Chemosphere 264:128580
10. Saha J, Begum A, Mukherjee A, Kumar S (2017) A novel green synthesis of silver nanoparticles and their catalytic action in reduction of Methylene Blue dye. Sustain Environ Res 27(5):245–250
11. Mohanta YK, Panda SK, Syed A, Ameen F, Bastia AK, Mohanta TK (2018) Bio-inspired synthesis of silver nanoparticles from leaf extracts of *Cleistanthus collinus* (Roxb.): Its potential antibacterial and anticancer activities. IET Nanobiotechnol 12(3):343–348
12. Dubey SP, Lahtinen M, Särkkä H, Sillanpää M (2010) Bioprospective of *Sorbus aucuparia* leaf extract in development of silver and gold nanocolloids. Colloid Surf B: Biointerfaces 80(1):26–33
13. Suvith VS, Philip D (2014) Catalytic degradation of methylene blue using biosynthesized gold and silver nanoparticles. Spectrochim Acta - A: Mol Biomol Spectrosc 118:526–532
14. Rajasekar R, Samuel M, Edison TNJI, Raman N (2021) Sustainable synthesis of silver nanoparticles using *Alstonia scholaris* for enhanced catalytic degradation of methylene blue. J Mol Struct 1246:131208
15. Safdar M, Qumar GM, Saravanan M, Khailany RA, Ozaslan M, Gondal MA, Deekonda K, Shahzad Q, Junejo Y (2019) Synthesis and characterization of Cefditoren capped silver nanoparticles and their antimicrobial and catalytic degradation of Ibuprofen. J Clust Sci 30:1663–1671
16. Ameen F, Abdullah MM, Al-Homaidan AA, Al-Lohedan HA, Al-Ghanayem AA, Almanso A (2020) Fabrication of silver nanoparticles employing the cyanobacterium *Spirulina platensis* and its bactericidal effect against opportunistic nosocomial pathogens of the respiratory tract. J Mol Struct 1217:128392
17. Wasilewska A, Klekotka U, Zambrzycka M, Zambrowski G, Święcicka I, Kalska-Szostko B (2023) Physico-chemical properties and antimicrobial activity of silver nanoparticles fabricated by green synthesis. Food Chem 400:133960
18. Dağlıoğlu Y, Yavuz MC, Ertürk O, Ameen F, Khatami M (2023) Investigation of cell damage of periodontopathic bacteria exposed to silver, zirconium oxide, and silicon oxide nanoparticles as antibacterial agents. Micro Nano Lett 18(9–12):12178
19. Yu SJ, Yin YG, Liu JF (2013) Silver nanoparticles in the environment. Environ Sci Process Impacts 15(1):78–92
20. Karuppiah C, Palanisamy S, Chen SM, Emmanuel R, Ali MA, Muthukrishnan P, Al-Hemaid FM (2014) Green biosynthesis of silver nanoparticles and nanomolar detection of p-nitrophenol. J Solid State Electrochem 18:1847–1854
21. Das TK, Ghosh SK, Das NC (2023) Green synthesis of a reduced graphene oxide/silver nanoparticles-based catalyst for degradation of a wide range of organic pollutants. Nano-Struct Nano-Objects 34:100960
22. Kumaresan M, Kannan M, Sankari A, Chandrasekhar CN, Vasanthi D (2019) Phytochemical screening and antioxidant activity of *Jasminum multiflorum* (pink Kakada) leaves and flowers. J Pharmacogn Phytochem 8(3):1168–1173
23. Filho ACD, de Jesus SJ, Carriço MRS, Viçozi GP, Flores WH, Denardin CC, Denardin ELG (2023) Green synthesis silver nanoparticles *Bougainvillea glabra* Choisy/LED light with high catalytic activity in the removal of methylene blue aqueous solution. Environ Sci Pollut Res 30(13):36244–36258
24. Zhang W, Tan F, Wang W, Qiu X, Qiao X, Chen J (2012) Facile, template-free synthesis of silver nanodendrites with high catalytic activity for the reduction of p-nitrophenol. J Hazard Mater 217:36–42
25. Das TK, Remanan S, Ghosh S, Ghosh SK, Das NC (2021) Efficient synthesis of catalytic active silver nanoparticles illuminated cerium oxide nanotube: a mussel inspired approach. Environ Nanotechnol Monit Manag 15:100411
26. Junejo Y, Safdar M, Akhtar MA, Saravanan M, Anwar H, Babar M, Babar ME (2019) Synthesis of tobramycin stabilized silver nanoparticles and its catalytic and antibacterial activity against pathogenic bacteria. J Inorg Organomet Polym Mater 29:111–120
27. Huang J, Li Q, Sun D, Lu Y, Su Y, Yang X, Chen C (2007) Biosynthesis of silver and gold nanoparticles by novel sundried *Cinnamomum camphora* leaf. Nanotechnol 18(10):105104
28. Narayanan KB, Park HH, Sakthivel N (2013) Extracellular synthesis of mycogenic silver nanoparticles by *Cylindrocladium floridanum* and its homogeneous catalytic degradation of 4-nitrophenol. Spectrochim Acta - A: Mol Biomol Spectrosc 116:485–490
29. Vidhu VK, Aromal SA, Philip D (2011) Green synthesis of silver nanoparticles using *Macrotyloma uniflorum*. Spectrochim Acta - A: Mol Biomol Spectrosc 83(1):392–397
30. Saygılı T, Kahraman HT, Aydın G, Avcı A, Pehlivan E (2023) Production of PLA-based AgNPs-containing nanofibers by electrospinning method and antibacterial application. Polym Bull 1–18
31. Guajardo-Pacheco MJ, Morales-Sánchez JE, González-Hernández J, Ruiz F (2010) Synthesis of copper nanoparticles using soybeans as a chelant agent. Mater Lett 64(12):1361–1364
32. Azizi M, Azimzadeh M, Afzali M, Alafzadeh M, Mirhosseini SH (2018) Characterization and optimization of using *Calendula offlcinalis* extract in fabrication of polycaprolactone-gelatin electrospun nanofibers for wound dressing applications. J Adv Mater Proc 6(2):34–46
33. Bar H, Bhui DK, Sahoo GP, Sarkar P, Pyne S, Misra A (2009) Green synthesis of silver nanoparticles using seed extract of *Jatropha curcas*. Colloids Surf A Physicochem Eng Aspects 348(1–3):212–216
34. Philip D, Unni C (2011) Extracellular biosynthesis of gold and silver nanoparticles using Krishna tulsi (*Ocimum sanctum*) leaf. Physica E Low Dimens Syst Nanostruct 43(7):1318–1322
35. Ameen F, AlYahya SA, Bakhrebah MA, Nassar MS, Aljuraifani A (2018) Flavonoid dihydromyricetin-mediated silver nanoparticles as potential nanomedicine for biomedical treatment of infections caused by opportunistic fungal pathogens. Res Chem Intermed 44:5063–5073
36. Ameen F, Alown F, Al-Owaidi MF, Sivapriya T, Ramírez-Coronel AA, Khat M, Akhavan-Sigari R (2023) African plant-mediated for

biosynthesis silver nanoparticles and evaluation of their toxicity, and antimicrobial activities. S Afr J Bot 156:213–222
37. Almansob A, Bahkali AH, Albarrag A, Alshomrani M, Binjomah A, Hailan WA, Ameen F (2022) Effective treatment of resistant opportunistic fungi associated with immuno-compromised individuals using silver biosynthesized nanoparticles. Appl Nanosci 12(12):3871–3882
38. Manosalva N, Tortella G, Cristina Diez M, Schalchli H, Seabra AB, Durán N, Rubilar O (2019) Green synthesis of silver nanoparticles: effect of synthesis reaction parameters on antimicrobial activity. World J Microbiol Biotechnol 35:1–9
39. Dong C, Chuanliang C, Zhang X, Zhang Y, Wang X, Yang X, Zhou K, Xiao X, Yuan B (2017) Wolfberry fruit (*Lycium barbarum*) extract mediated novel route for the green synthesis of silver nanoparticles. Optik 130:162–170
40. Aziz W, Jassim HA (2018) A novel study of pH influence on Ag nanoparticles size with antibacterial and antifungal activity using green synthesis. World Sci News 97:139–152
41. Kadam J, Dhawal P, Barve S, Kakodkar S (2020) Green synthesis of silver nanoparticles using cauliflower waste and their multifaceted applications in photocatalytic degradation of methylene blue dye and Hg 2+ biosensing. SN Appl Sci 2:1–16
42. Arya G, Kumari RM, Gupta N, Kumar A, Chandra R, Nimesh S (2018) Green synthesis of silver nanoparticles using Prosopis juliflora bark extract: reaction optimization, antimicrobial and catalytic activities. Artif cells Nanomed Biotechnol 46(5):985–993
43. Qasim Nasar M, Zohra T, Khalil AT, Saqib S, Ayaz M, Ahmad A, Shinwari ZK (2019) *Seripheidium quettense* mediated green synthesis of biogenic silver nanoparticles and their theranostic applications. Green Chem Lett Rev 12(3):310–322
44. Edison TJI, Sethuraman MG (2012) Instant green synthesis of silver nanoparticles using *Terminalia chebula* fruit extract and evaluation of their catalytic activity on reduction of methylene blue. Process Biochem 47(9):1351–1357
45. Joshi SJ, Geetha SJ, Al-Mamari S, Al-Azkawi A (2018) Green synthesis of silver nanoparticles using pomegranate peel extracts and its application in photocatalytic degradation of methylene blue. Jundishapur J Nat Pharm Prod 13(3)
46. Hachemaoui M, Mokhtar A, Ismail I, Mohamedi MW, Iqbal J, Taha I, Boukoussa B (2021) M (M: Cu Co, Cr or Fe) nanoparticles-loaded metal-organic framework MIL-101 (Cr) material by sonication process: catalytic activity and antibacterial properties. Microporous Mesoporous Mater 323:111244
47. Asli B, Abdelkrim S, Zahraoui M, Mokhtar A, Hachemaoui M, Bennabi F, Boukoussa B (2022) Catalytic reduction and antibacterial activity of MCM-41 modified by silver nanoparticles. Silicon 14(18):12587–12598
48. Alula MT, Lemmens P, Madiba M, Present B (2020) Synthesis of free-standing silver nanoparticles coated filter paper for recyclable catalytic reduction of 4-nitrophenol and organic dyes. Cellul 27:2279–2292
49. Das TK, Ganguly S, Remanan S, Ghosh S, Das NC (2020) Mussel-inspired Ag/poly (norepinephrine)/MnO 2 heterogeneous nanocatalyst for efficient reduction of 4-nitrophenol and 4-nitroaniline: an alternative approach. Res Chem Intermed 46:3629–3650
50. Otari SV, Patil RM, Nadaf NH, Ghosh SJ, Pawar SH (2014) Green synthesis of silver nanoparticles by microorganism using organic pollutant: its antimicrobial and catalytic application. Environ Sci Pollut Res 21:1503–1513
51. Pradhan N, Pal A, Pal T (2001) Catalytic reduction of aromatic nitro compounds by coinage metal nanoparticles. Langmuir 17(5):1800–1802
52. Singh J, Mehta A, Rawat M, Basu S (2018) Green synthesis of silver nanoparticles using sun dried tulsi leaves and its catalytic application for 4-Nitrophenol reduction. J Environ Chem Eng 6(1):1468–1474
53. Das TK, Das NC (2022) Advances on catalytic reduction of 4-nitrophenol by nanostructured materials as benchmark reaction. Int Nano Lett 12(3):223–242
54. Somasundaram CK, Atchudan R, Edison TNJI, Perumal S, Vinodh R, Sundramoorthy AK, Lee YR (2021) Sustainable synthesis of silver nanoparticles using marine algae for catalytic degradation of methylene blue. Catalysts 11(11):1377
55. Rohaizad A, Shahabuddin S, Shahid MM, Rashid NM, Hir ZAM, Ramly MM, Aspanut Z (2020) Green synthesis of silver nanoparticles from *Catharanthus roseus* dried bark extract deposited on graphene oxide for effective adsorption of methylene blue dye. J Environ Chem Eng 8(4):103955
56. Akilandaeaswari B, Muth K (2021) One-pot green synthesis of Au-Ag bimetallic nanoparticles from *Lawsonia inermis* seed extract and its catalytic reduction of environmental polluted methyl orange and 4-nitrophenol. J Taiwan Inst Chem 127:292–301
57. Doan VD, Phan TL, Vasseghian Y, Evgenievna LO (2022) Efficient and fast degradation of 4-nitrophenol and detection of Fe (III) ions by *Poria cocos* extract stabilized silver nanoparticles. Chemosphere 286:131894
58. Ameen F, Amirul Islam M, Dhanker R (2022) Green synthesis of silver nanoparticles from vegetable waste of pea *Pisum sativum* and bottle gourd *Lagenaria siceraria*: characterization and antibacterial properties. Front Environmen Sci 10:941554
59. Muhammad G, Hussain MA, Amin M, Hussain SZ, Hussain I, Bukhari SNA, Naeem-ul-Hassan M (2017) Glucuronoxylan-mediated silver nanoparticles: green synthesis, antimicrobial and wound healing applications. RSC Adv 7(68):42900–42908
60. Sharma VK, Yngard RA, Lin Y (2009) Silver nanoparticles: green synthesis and their antimicrobial activities. Adv Colloid Interface Sci 145(1–2):83–96
61. Morones JR, Elechiguerra JL, Camacho A, Holt K, Kouri JB, Ramírez JT, Yacaman MJ (2005) The bactericidal effect of silver nanoparticles. Nanotechnol 16(10):2346